NJC

Accepted Manuscript

This article can be cited before page numbers have been issued, to do this please use: Y. Yue, D. Wu, S. Zeng, M. Yang, H. Wang and J. Lu, *New J. Chem.*, 2017, DOI: 10.1039/C7NJ00844A.

ROYAL SOCIETY OF CHEMISTRY

rsc.li/njc

View Article Online
DOI: 10.1039/C7NJ00844A

Journal Name

LETTER

Alkaloid-induced asymmetric hydrogenation on bimetallic Pt@Cu cathodes by electrochemical conditions†

Received 00th January 20xx,
Accepted 00th January 20xx

DOI: 10.1039/x0xx00000x

www.rsc.org/

Ying-Na Yue, Di Wu, Sheng Zeng, Man-Ping Yang, Huan Wang* and Jia-Xing Lu*

Bimetallic Pt@Cu nanoparticles (NPs) with low Pt weight ratio loading obtained by reducing platinum precursors on Cu NPs were coated on carbon paper and used as a cathode for asymmetric hydrogenation by the electrochemical method. The Pt@Cu NPs exhibited enhanced catalytic performance in ketone electrohydrogenation. The enantioselective electrohydrogenation of pro-chiral aromatic ketones (2,2,2-trifluoroacetophenone, acetophenone, 2-phenylacetone, 4-methylacetophenone) induced by cinchonidine alkaloids was investigated in an undivided cell to obtain optically active alcohols. Optically active α-(trifluoromethyl) benzyl alcohols with 59% enantiomeric excess value and 25% yield were obtained. All experimental procedures were performed under mild conditions, that is, without the utilization of high temperature and pressure. The Pt@Cu NPs showed excellent stability and reusability.

Introduction

Chirality is one of the basic attributes of nature and life. Recently, the close relationship between asymmetric synthesis and pharmaceutical, agrochemical, and materials science has shown important application prospects.[1] Asymmetric hydrogenation provides an effective way to produce chiral drugs and plays an important role in asymmetric synthesis. Although most asymmetric homogeneous catalysts, such as Rh, Ir and Ru complexes, are noble metal catalyst that are highly effective in asymmetric catalysis, these noble metals are rare and expensive.[2-6] The reported work on "modified catalysts" has opened a new field in the development of chiral heterogeneous catalytic systems. Take for example the metallic Pt-cinchona system; this system shows high performance in the hydrogenation of α-ketoesters with excellent yields of corresponding chiral alcohols with high enantiomeric excess (ee) values,[7-11] although high-pressure hydrogen is required in such a conventional asymmetric system.

In recent years, electrochemical techniques have become an appropriate method in organic synthesis, and they are known to be green under mild conditions. According to our reported research studies,[12-15] alkaloids could be electrosorbed on metal cathodes for the asymmetric electroreduction of aromatic ketones. Suitable yields and ee values are obtained under mild conditions. Nevertheless, the yields and ee values of the asymmetric scheme are still unsatisfactory.

Pt is recognized as an excellent metal to adsorb alkaloids for asymmetric electrohydrogenation, but this noble metal is sparse and expensive. In our work, Pt@Cu nanoparticles (NPs) with low Pt loading are prepared to reduce the cost of catalysts. The electrocatalytic properties of Pt@Cu NPs for asymmetric hydrogenation are explored under the guidelines of this strategy.

Experimental

Preparation of Cu NPs and Pt@Cu NPs

In the present work, 1.2 g of $Cu(NO_3)_2 \cdot 3H_2O$ is dissolved in 50 mL of deionized (DI) water. Then, 6 g of polyvinyl pyrrolidone (PVP) is added to the solution. After stirring for 10 min, 50 mL of hydrazine hydrate solution (10%) and 2 mL of ethylenediamine are slowly added to the solution. The mixture is then stirred at 30 °C for 3 h. Cu NPs (Fig. S1, ESI †) are precipitated immediately. The precipitate is filtered, washed thrice with 20 mL of DI water, and dried for 8 h under vacuum.

The synthesis of Pt@Cu NPs is performed as follows. Cu NPs are stably suspended in DI water through supersonic dispersion. A certain concentration of $H_2PtCl_6 \cdot 6H_2O$ solution is added in a Cu homogeneous slurry. The mixture is then stirred at 25 °C for 2 h. Pt is precipitated on Cu NPs immediately. The precipitate is filtered, washed thrice with 20 mL of DI water, and dried for 8 h under vacuum.

Material characterization

Shanghai Key Laboratory of Green Chemistry and Chemical Processes, School of Chemistry and Molecular Engineering, East China Normal University, Shanghai, 200062, China. E-mail: hwang@chem.ecnu.edu.cn, jxlu@chem.ecnu.edu.cn; Tel: +86 21-52134935, +86 21-62233491

† Electronic Supplementary Information (ESI) available: Characterization of Cu NPs, and Pt@Cu-2 NPs after use. See DOI: 10.1039/x0xx00000x

View Article Online
DOI: 10.1039/C7NJ00844A

Transmission electron microscope (TEM) images are captured with an FEI Tecnai G^2 F30 microscope operated at 300 kV. Scanning electron microscope (SEM) images are captured with a Hitachi S-4800 microscope. X-ray diffraction (XRD) patterns are recorded with an Ultima IV X-ray powder diffractometer with Cu Kα radiation (k = 1.5406 Å). The element content is measured with inductive coupled plasma (ICP) emission spectrometer. Nitrogen adsorption-desorption isotherms and Brunauer-Emmett-Teller (BET) surface areas are measured with a Belsorp-Max analyzer at 77 K. All reagents are used as received.

Cyclic voltammetry

Cyclic voltammograms are measured with the CHI 600c Electrochemical Station (Shanghai Chenhua Instruments Company). The working electrode is fabricated as follows. Exactly 10 mg of Pt@Cu NPs is dispersed in 60 µL of mixed solution containing DI water and carboxymethylcellulose sodium (60 mg). Then, 10 µL of the Pt@Cu colloid is dropped onto the surface of a glassy carbon (GC) electrode and dried at room temperature. The counter and reference electrodes are a Pt net (1 cm × 1 cm) and an Ag/AgI/I^- electrode, respectively. All the electrochemical measurements are performed at a scan rate of 0.1 V s^{-1} in N_2 saturated solution.

Galvanostatic electrohydrogenation

Galvanostatic eletrohydrogenation is performed with a direct-current-regulated power supply (HY3002D, HYelec®, China). The Pt@Cu colloid is coated on carbon paper (2 cm × 2 cm) and used as a cathode. The yield and ee value (calculated as Eq. S1, ESI†) of the product are determined with Shimadzu GC-2010 equipped with a Stabilwax column (30 m × 0.32 mm i.d., 0.5 µm film thickness). Typical galvanostatic electroreduction is conducted in a mixture of 0.1 M 2,2,2-trifluoroacetophenon, 3 mM cinchonidine (CD) and 0.1 M tetraethylammonium iodide (TEAI) in 20 mL of co-solvent (MeCN/n-amyl alcohol=1/1) in an undivided glass cell with the Pt@Cu cathode and sacrificial magnesium (Mg) anode.

Results and discussion

The Pt@Cu NPs are prepared with different ratios of Pt and then labelled as Pt@Cu-1, Pt@Cu-2 and Pt@Cu-3 accordingly. As shown in Figs. 1 A-C, the typical SEM patterns display the overall morphology of the Pt@Cu NPs, which show an average size of 55 nm. Surprisingly, the XRD patterns of the Pt@Cu NPs only show the diffraction peaks of Cu and not the typical diffraction peaks of metallic Pt as observed by comparing the XRD patterns of pure Cu, and the Pt@Cu NPs (Fig. 1D). Thus, the prepared Pt@Cu NPs are further characterized by TEM.

The low-magnification TEM images of Pt@Cu-1 (Fig. 2A), Pt@Cu-2 (Fig. 2B), and Pt@Cu-3 (Fig. 2C) indicate that the Pt nanoparticles disperse on the Cu nanoparticles in comparison with the pure Cu NPs (Fig. S2, ESI†). The high-magnification TEM image of Pt@Cu-2 in Fig. 2D shows lattice spacings of 2.26 and 2.09 Å for the (111) planes of face-centered cubic Pt and Cu, respectively. In the preparation of Pt@Cu NPs, platinum precursors are reduced by the superficial copper, and small Pt islands form on the surface of the Cu NPs. The distribution of Pt NPs is confirmed via the high-angle annular dark-field scanning TEM (HADDF-STEM) mapping (Fig. 2E), which shows that Pt nanoparticles are dispersed uniformly on the Cu nanoparticles.

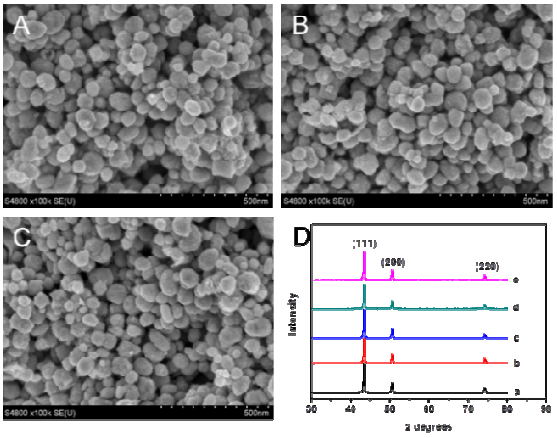

Fig. 1 SEM patterns of Pt@Cu-1 (A), Pt@Cu-2 (B), Pt@Cu-3 (C); (D) XRD patterns of Pt@Cu-1 (a), Pt@Cu-2 (b) , Pt@Cu-3 (c), pure Cu NPs (d), Pt@Cu-2 NPs after stability test (e).

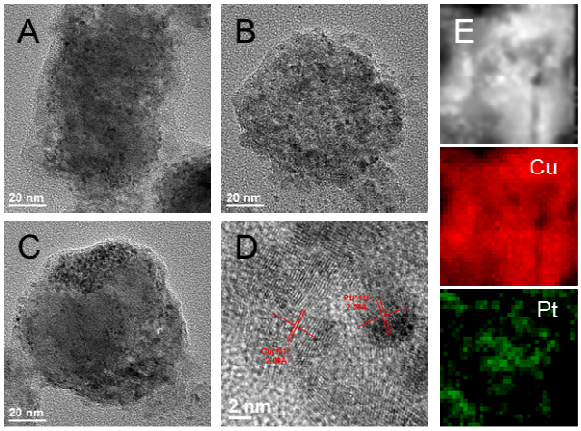

Fig. 2 Low magnification TEM image of the overall morphology of Pt@Cu-1 (A), Pt@Cu-2 (B) and Pt@Cu-3 (C). High-resolution TEM image (D) and HADDF-STEM elemental mapping (E) of Pt@Cu-2.

The ratios of Pt in the Pt@Cu NPs, which are extensively identified using ICP, are 2.1, 2.6 and 3.1 wt% for Pt@Cu-1, Pt@Cu-2 and Pt@Cu-3 respectively. The nitrogen adsorption-desorption isotherm shows that Pt@Cu-2 NPs has a specific surface area of 40.6 m^2 g^{-1}, which is larger than those of Pt@Cu-1 NPs and Pt@Cu-3 NPs, for pure Cu NPs, the specific surface area is only 6.0 m^2 g^{-1} (Fig. S3 and Table S1, ESI†). The specific surface area increases after the Pt NPs anchor onto the surface of pure Cu NPs.

Aside from preparing and characterizing the Pt@Cu NPs, we pay close attention to their electrocatalytic properties in asymmetric hydrogenation. The cyclic voltammograms (Fig. 3) show two reduction peaks at −1.1 and −1.8 V, of 2,2,2-

View Article Online
DOI: 10.1039/C7NJ00844A

trifluoroacetophenon on Pt@Cu/GC, pure Cu NPs/GC, and pure Pt NPs/GC. These reduction peaks correspond to the two-electron transfer of the ketone group (C=O). At the same time, the peak currents on the pure Cu NPs/GC and Pt NPs/GC are both lower than those on Pt@Cu/GC. This result indicates that the Pt@Cu NPs are more efficient in the electroreduction of substrates.

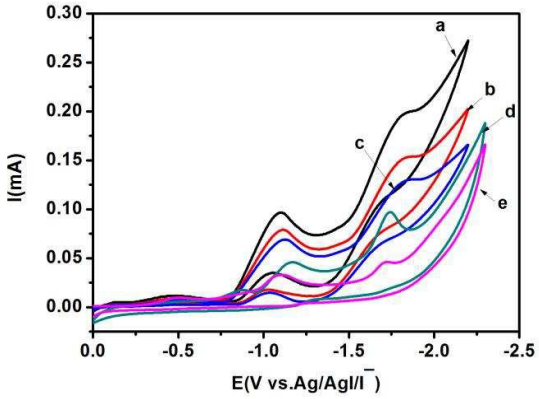

Fig. 3 Cyclic voltammograms of 10 mM 2,2,2-trifluoroacetophenon in MeCN/n-amyl alcohol (1/1, volume ratio)-0.1 M TEAI with the scan rate of 0.1 V s^{-1} on different electrodes: Pt@Cu-2/GC (a), Pt@Cu-3/GC (b), Pt@Cu-1/GC (c), Pt NPs/GC (d), Cu NPs/GC (e), T = 25°C.

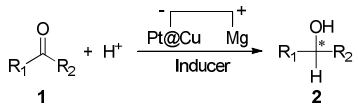

	R_1	R_2
a	Ph	CF_3
b	Ph	Me
c	Bn	Me
d	Tol	Me

Scheme. 1 Enantioselective electrohydrogenation of aromatic ketones.

For the asymmetric hydrogenation of aromatic ketones (as shown in **Scheme 1**), the carbon paper coated with Pt@Cu-2 powder is used as a cathode with a sacrificial magnesium (Mg) anode. CD was added into the solution as an inducer. Optically active α-(trifluoromethyl) benzyl alcohol (**2a**) is obtained with 59% ee value and 25% yield under constant current electrolysis at 5 °C (Table 1, entry 2). Racemic product is detected with no chiral inducer CD (Table 1, entry 3), indicating that the chiral inducer is crucial in this asymmetric electrosynthesis. That is, the chiral inducer is adsorbed on the electrode surface to create a chiral environment for asymmetric induction.[16] To compare the catalytic abilities of the different cathode materials in our current system, we use Pt@Cu-1, Pt@Cu-3, Pt net, Cu, and pure Cu NPs as cathodes. When Cu and pure Cu NPs are used as cathodes, racemic products are also detected (Table 1, entries 6-7), indicating that Cu and Cu NPs cannot catalyze the configuration transition of **1a** effectively. As CD is adsorbed on Pt (111),[17] chiral product with 6% and 28% ee values could be obtained on Pt and Pt NPs, respectively (Table 1, entries 5 and 7). Significantly high ee values are obtained on Pt@Cu-1, Pt@Cu-2, and Pt@Cu-3 (Table 1, entries 1-2, 4). The higher catalytic activity of Pt@Cu in comparison with that of pure Cu NPs and Pt NPs proves the advantage of such bimetal. The enhanced activity and selectivity are due to the exposed active site and the synergistic effect between Cu and Pt. The Cu atoms in the core domain coherently match the lattice structures of the exterior Pt islands (Fig. 2D), resulting in the formation of the inserted pseudo-Cu-Pt alloy heterointerface.[18, 19] The pseudo-heterointerface is favorable for reducing the electronic binding energy in Pt and facilitating hydrogenation reduction. Furthermore, the many atomic steps exposed on the Pt island surface (Fig. 2D) can act as highly active sites for enantioselective hydrogenation reaction.[18, 20, 21] Among the three types of Pt@Cu NPs, Pt@Cu-2 shows the highest ee value and yield, which agrees with the cyclic voltammogram of **1a** (Fig. 3). The different ee value and yield of **2a** on Pt@Cu cathodes could be explained by two factors: the ratios of Pt in the Pt@Cu NPs and the dispersity of Pt particles on the Cu particles. The ratios of Pt in Pt@Cu-1 are the lowest, and thus, CD could not be sufficiently adsorbed on this material. However, excessive Pt causes the aggregation of the NPs for Pt@Cu-3, as shown in Fig. 2C. This condition also limits the adsorption of CD. By contrast, Pt@Cu-2 has a relatively appropriate ratio of Pt. Thus, it represents the highest electrocatalytic ability for asymmetric electrosynthesis.

The effect of temperature on asymmetric synthesis is always significant. Therefore, we investigate a series of asymmetric electroreductions of **1a** from −20 °C to 25 °C. As shown in Table 1 (entries 2, 8-18), the ee value increases from 16% to 89% as the temperature decreases. At the same time, the alcohol yield decreases. A low temperature slows down the reaction rate, thereby influencing electron transfer and asymmetric induction. For heterogeneous asymmetric hydrogenation, high reaction temperatures are detrimental to achieving a high ee due to the subtle energetic differences (few kJ mol^{-1}) related to the enantiodifferentiating process.[22] The same may also be suitable for asymmetric electroreduction.

As a result of the suitable outcomes obtained with **1a**, the catalytic performance of Pt@Cu NPs on different substrates is tested under the reaction conditions presented in Table 1, entry 2. Optically active **2b** is obtained with 39% ee value and 17% yield; both values are better than the reported results (28% ee value and 6% yield on Cu nanoparticle cathode and 28% ee value and 5% yield on CD@Cu cathode).[23, 24] The bimetallic NPs show universal catalytic performance in the asymmetric hydrogenation of the substituted ketones, such as **1c** and **1d**. Therefore, Pt@Cu NPs catalyze the asymmetric electrohydrogenation of carbonyl induced by alkaloids effectively with several types of substrates.

The reusability of Pt@Cu-2 is subsequently examined in the asymmetric hydrogenation of **1a** under the reaction conditions detailed in Table 1, entry 2. The yield and ee value of **2a** could be maintained at approximately 24% and 57%, respectively, for six times at least (Fig. 4). To explore the stability of the catalyst, Pt@Cu-2 used for six times is characterized via SEM (Fig. S4, ESI†) and TEM (Fig. S5, ESI†). Pt@Cu-2 retains its

View Article Online
DOI: 10.1039/C7NJ00844A

Table1 Electrocatalytic asymmetric hydrogenation of ketones[a]

Entry	Cathode	Substrate	T (°C)	Yield[b] (%)	R-ee[b] (%)
1	Pt@Cu-1	**1a**	5	21	47
2	Pt@Cu-2	**1a**	5	25	59
3[c]	Pt@Cu-2	**1a**	5	64	0
4	Pt@Cu-3	**1a**	5	16	50
5	Pt	**1a**	5	16	6
6	Cu	**1a**	5	12	0
7	Pt NPs	**1a**	5	19	28
8	Cu NPs	**1a**	5	14	0
9	Pt@Cu-2	**1a**	25	54	16
10	Pt@Cu-2	**1a**	20	46	19
11	Pt@Cu-2	**1a**	15	36	25
12	Pt@Cu-2	**1a**	10	27	33
13	Pt@Cu-2	**1a**	7.5	26	44
14	Pt@Cu-2	**1a**	2.5	14	63
15	Pt@Cu-2	**1a**	0	6	71
16	Pt@Cu-2	**1a**	-5	5	78
17	Pt@Cu-2	**1a**	-10	5	83
18	Pt@Cu-2	**1a**	-15	4	87
19	Pt@Cu-2	**1a**	-20	3	89
20	Pt@Cu-2	**1b**	5	17	39
21	Pt@Cu-2	**1c**	5	5	23
22	Pt@Cu-2	**1d**	5	18	41

[a] Anode: Mg, 20 mL co-solvent (MeCN/n-amyl alcohol=1/1), 0.1 M substrate: **1a**, supporting electrolyte: 0.1 M TEAI, inducer: 3 mM CD, current density: 2 mA cm^{-2}, charge: 2 F mol^{-1}. [b] Determined by GC with a chiral column. [c] With no CD.

particle morphology after being used for six times, and only a small portion of particles agglomerates into large ones. In addition, no phase separation occurs between Pt NPs and Cu NPs. The XRD patterns of Pt@Cu-2 NPs before and after being used for six times show no significant differences in the stability test (curve e in Fig. 1D). Therefore, the Pt@Cu NP electrode prepared in this work is reusable and stable, thereby exhibiting potential for practical applications.

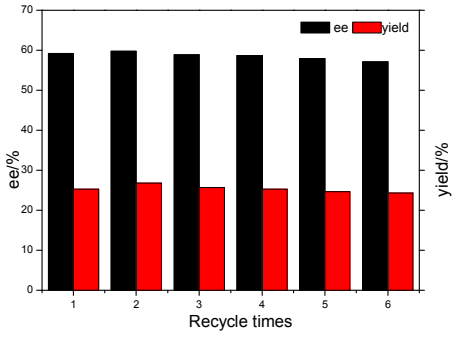

Fig. 4 Reuse of the Pt@Cu-2 NPs cathode. Reaction condition as given in Table 1, entry 2.

Conclusions

Pt@Cu NPs with different Pt weight ratios are synthesized. As a result, these NPs show high catalytic activity and stability for the asymmetric hydrogenation of 2,2,2-trifluoroacetophenon. High temperature and pressure are not applied in the preparation of Pt@Cu NPs and the electroreduction of aromatic ketones. All experimental procedures are performed under mild conditions. Moreover, Pt@Cu NPs sustain high activity after recycling for six times. Pt@Cu NPs could be used as excellent electrocatalysts due to their large surface area, good stability, favorable reusability and high conductivity.

Acknowledgements

Financial support from National Natural Science Foundation of China (21373090, 21473060, 21673078) is gratefully acknowledged.

Notes and references

1 R. Dalpozzo, *Chem. Soc. Rev.*, 2015, **44**, 742-778.
2 T. Punniyamurthy, M. Mayr, A. S. Dorofeev, C. J. R. Bataille, S. Gosiewska, B. Nguyen, A. R. Cowley and J. M. Brown, *Chem. Commun.*, 2008, 5092-5094.
3 J. H. Xie, S. F. Zhu and Q. L. Zhou, *Chem. Rev.*, 2011, **111**, 1713-1760.
4 Y. G. Zhou, *Acc. Chem. Res.*, 2007, **40**, 1357-1366.
5 C. S. Shultz and S. W. Krska, *Acc. Chem. Res.*, 2007, **40**, 1320-1326.
6 T. Yamamura, H. Nakatsuka, S. Tanaka and M. Kitamura, *Angew. Chem. Int. Ed.*, 2013, **52**, 9313-9315.
7 K. Szori, K. Balazsik, K. Felfoldi and M. Bartok, *J. Catal.*, 2006, **241**, 149-154.
8 K. Balazsik, K. Szori, K. Felfoldi, B. Torok and M. Bartok, *Chem. Commun.*, 2000, 555-556.
9 M. Sutyinszki, K. Szori, K. Felfoldi and M. Bartok, *Catal. Lett.*, 2002, **81**, 281-284.
10 B. Torok, K. Balazsik, M. Torok, K. Felfoldi and M. Bartok, *Catal. Lett.*, 2002, **81**, 55-62.
11 S. Diezi, S. Reimann, N. Bonalumi, T. Mallat and A. Baiker, *J. Catal.*, 2006, **239**, 255-262.
12 B. L. Chen, Y. Xiao, X. M. Xu, H. P. Yang, H. Wang and J. X. Lu, *Electrochim. Acta*, 2013, **107**, 320-326.
13 B. L. Chen, Z. Y. Tu, H. W. Zhu, W. W. Sun, H. Wang and J. X. Lu, *Electrochim. Acta*, 2014, **116**, 475-483.
14 S. F. Zhao, M. X. Zhu, K. Zhang, H. Wang and J. X. Lu, *Tetrahedron lett.*, 2011, **52**, 2702-2705.
15 K. Zhang, H. Wang, S. F. Zhao, D. F. Niu and J. X. Lu, *J. Electroanal. Chem.*, 2009, **630**, 35-41.
16 S. Baldanza, J. Ardini, A. Giglia and G. Held, *Surf. Sci.*, 2016, **643**, 108-116.
17 E. Schmidt, W. Kleist, F. Krumeich, T. Mallat and A. Baiker, *Chem. Eur. J.*, 2010, **16**, 2181-2192.
18 L. Wang, Y. Nemoto, Y. Yamauchi, *J. Am. Chem. Soc.*, 2011, **133**, 9674-9677.
19 M. Yamauchi, H. Kobayashi, H. Kitagawa, *ChemPhysChem*, 2009, **10**, 2566-2576.
20 S. W. Lee, S. Chen, W. Sheng, N. Yabuuchi, Y.-T. Kim, T. Mitani, E. Vescovo and Y. Shao-Horn, *J. Am. Chem. Soc.*, 2009, **131**, 15669-15677.
21 Z.-Y. Zhou, Z.-Z. Huang, D.-J. Chen, Q. Wang, N. Tian and S.-G. Sun, *Angew. Chem. Int. Ed.*, 2010, **49**, 411-414.
22 A. Baiker, *Chem. Soc. Rev.*, 2015, **44**, 7449-7464.
23 H. P. Yang, H. Wang and J. X. Lu, *Electrochem. Commun.*, 2015, **55**, 18-21.
24 H. P. Yang, Q. Fen, H. Wang and J. X. Lu, *Electrochem. Commun.*, 2016, **71**, 38-42.